POLITECNICO DI TORINO
Repository ISTITUZIONALE

Simultaneous improvement of ammonia mediated NOx SCR and soot oxidation for enhanced SCR-on-Filter application

(Article begins on next page)

03 July 2022

Simultaneous improvement of ammonia mediated NO$_x$ SCR and soot oxidation for enhanced SCR-on-Filter application

Authors:

Ferenc Martinovic[1], Tahrizi Andana[1], Marco Piumetti[1], Marco Armandi[1,2], Barbara Bonelli[1,2], Fabio Alessandro Deorsola*,[1], Samir Bensaid[1], Raffaele Pirone[1]

[1]Department of Applied Science and Technology, Politecnico di Torino, Corso Duca degli Abruzzi, 24, 10129 Torino (Italy)

[2]INSTM Unit of Torino-Politecnico, Corso Duca degli Abruzzi 24, 10129 Torino, Italy.

Corresponding Author:

* F.A. Deorsola

Department of Applied Science and Technology, Politecnico di Torino, Corso Duca degli Abruzzi 24, 10129 Torino, Italy

Tel.: +39 011 0904662; fax: +39 011 0904624; E-mail address: fabio.deorsola@polito.it

Abstract

The integration of NO_x reduction and catalytic soot oxidation was investigated for the SCRoF (Selective Catalytic Reduction on Filter) applications. By physically mixing a commercial SCR catalyst (either Fe-ZSM-5 and Cu-ZSM-5) with a soot oxidation catalyst (K/CeO_2-PrO_2), it was possible to lower the soot oxidation temperature by more than 150 degrees and, by optimizing the catalysts mass ratio in the mixture, NO_x conversion simultaneously increased, because NO oxidation induced a fast SCR reaction pathway, unlike during standard SCR. Such an improvement in NO_x conversion was more pronounced with the Fe-ZSM-5 than with the Cu-ZSM-5 zeolite, as the latter was more sensitive to the NO_2/NO_x ratio. In order to make the soot oxidation catalyst inactive towards ammonia oxidation, poisoning of the surface acid sites with 3.0 wt.% K_2CO_3 (corresponding to only 1.0 wt.% K) was performed. In the soot oxidation and SCR catalysts physical mixture, the soot was oxidized mainly by O_2 and the contribution of NO_2 to oxidation was negligible, as NO_2 itself was a key reactant in the (kinetically much faster) SCR reaction.

Keywords: SCR on Filter; soot oxidation; SCR; Fe-ZSM-5; Cu-ZSM-5.

1. Introduction

Diesel engines inherently have higher thermodynamic efficiency due to lean operation, which make them be preferred over petrol based internal combustion engines in long haul transport, locomotives, work machines, etc. Unfortunately, diesel engines have higher NO_x and soot emissions that are difficult to remove from the exhaust due to low temperature and net oxidizing conditions [1–3]. Due to the harmfulness of the exhaust gases, even more stringent emission limits are implemented with the latest Euro 6d, which is expected to come into force in 2020. To stay below threshold limits, especially those of NO_x and particulate matter (PM) emissions, aftertreatment of exhaust gasses is necessary [4,5].

Current aftertreatment systems are usually complex, expensive and require several successive reaction steps and monolith bricks. The main components are, typically, a diesel oxidation catalyst (DOC) for both NO and hydrocarbon oxidation, a catalyzed or non-catalyzed diesel particulate filter (DPF) for PM removal and a component for selective catalytic reduction (SCR) of NO_x [5–8]. NO_x SCR is mediated by a reductant, which is commonly ammonia (NH_3) obtained from the decomposition of urea in aqueous solution and Cu- or Fe-zeolites are currently the most efficient catalysts [9–13].

The main reactions occurring in aftertreatment systems are:

$2NO + 2NH_3 + 1/2O_2 \rightarrow 2N_2 + 3H_2O$ Standard SCR (R1)

$NO + NO_2 + 2NH_3 \rightarrow 2N_2 + 3H_2O$ Fast SCR (R2)

$6NO_2 + 8NH_3 \rightarrow 7N_2 + 12H_2O$ NO_2 SCR (R3)

$NO + 1/2O_2 \rightarrow NO_2$ NO oxidation (R4)

$NH_3 + O_2 \rightarrow xN_2O + xNO + xN_2$ Non selective ammonia oxidation (R5)

$C + O_2 \rightarrow xCO + xCO_2$ Soot oxidation with oxygen (R6)

$C + NO_2 + O_2 \rightarrow xCO + xCO_2 + NO$ NO_x assisted soot oxidation (R7)
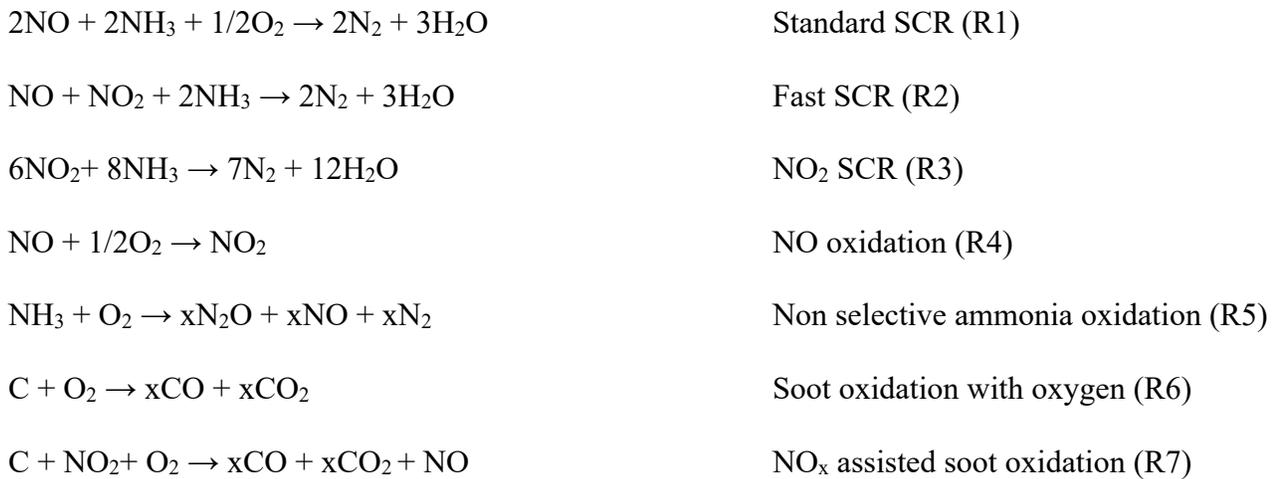
One method to reduce complexity and cost and to improve efficiency of aftertreatment systems is to integrate the DPF and the NO_x SCR into a single device, which is called a SCR on Filter (SCRoF) device. In a SCRoF, the SCR catalyst is washcoated on the pores of a monolith and the channels are plugged on alternating ends, to force exhaust gases through the wall, thereby performing simultaneously SCR and soot filtration. By this way, both size and cost are reduced and, if it is in close-coupled position, higher operating temperatures and more efficient performance can be achieved [11,13–19]. Several experimental and modeling studies has proven that passive soot oxidation is inhibited on SCRoF, as the fast SCR reaction (R2) is consuming the produced NO_2, which becomes unavailable for soot oxidation [11,13–19]. As soot accumulates during filtration, both resistance to the flow and pressure drop increase and the filter has to be regenerated by an active method whereby fuel is injected to increase the

temperature above 600 °C to oxidize all the soot [11,13–19]. Such regeneration is usually performed less frequently (or completely avoided) in DPF, as they are typically coated with a Pt-based NO oxidation catalyst, as NO_2 can passively oxidize soot at much lower temperature (< 400 °C) as compared to O_2 [1]. The high temperatures reached during regeneration can easily damage the filter and deactivate the SCR catalyst. For this reason, typically Fe and Cu zeolites are used for SCRoF application, as they present high hydrothermal stability and, to some extent, can withstand the harsh conditions of regeneration [11,13–19].

To decrease the frequency of filter regeneration, the NO_2/NO_x ratio should be adjusted above the ideal value of 0.5 required for SCR. The rationale is that part of the excess NO_2 will be consumed by the accumulated soot, the NO_2/NO_x ratio self-regulating back to 0.5 [11,13,14]. Another idea is to concentrate the SCR catalyst in the downstream part of the monolith, with NO_x being available for soot oxidation in the inlet side [11,18]. Such partial solutions, however, do not solve the problem of soot accumulation and regeneration, merely delaying with it.

Here, a novel physical mixture of an SCR catalyst and soot oxidation catalyst is proposed as a solution to soot accumulation. So far, some physical mixtures of quite different catalysts have been applied for NO_x reduction in various and quite innovative settings, such as Ag/Al_2O_3 combined with Sn/Al_2O_3 or Zn-ZSM-5 for Hydrocarbon (HC)-SCR [20,21], Pt/Al_2O_3 and Cu-Zn-Al water-gas shift to generate in situ hydrogen for NO_x reduction [22], combination of Fe and Cu zeolites to widen the SCR window [12,23] and combination of Lean NO_x Trap (LNT) and SCR catalysts for in situ ammonia generation and utilization in the so-called "urealess passive SCR" [24,25]. Another concept introduced in 1997 by Misono et al. [26] is to combine a catalyst for NO oxidation (R4) with an SCR catalyst and transform the reaction pathway from standard SCR (R1) to fast SCR (R2) whereby higher NO_x conversion can be achieved. A similar concept was later investigated in more detail by the research groups of Stakheev et al. [27–29] and Salazar et. al. [30,31], where mainly Mn was the NO oxidation catalyst. One important

finding, emphasized even in the references [26–31], was that NO_x conversion was enhanced only at low temperatures, and decreased significantly above 300 °C. The reason was that the oxidative component oxidized not only NO, but also NH_3 (the reductant) producing high amounts of N_2O and thus, as ammonia was depleted, the SCR reaction could not proceed. For this reason, we tailored the soot oxidation catalyst specifically to be selectively oxidative towards both soot and NO, to simultaneously improve soot oxidation and NO_x conversion by transforming the reaction pathway from standard to fast SCR. An innovative solution was found to prevent ammonia oxidation, whereby the catalyst was impregnated with a reasonably small amount of potassium (ca. 8.0 wt%) [32]. Potassium selectively poisoned the acid sites and the catalyst became passive towards ammonia oxidation, while simultaneously soot oxidation was improved.

The aim of this work is to investigate the integration of soot oxidation and NO_x SCR by a two-component selective catalytic system and to investigate the interaction between them. Particularly, the novel solution proposed here is a physical mixture of two different catalysts, namely a SCR catalyst and a soot oxidation catalyst, in order to achieve the combined effect. As SCR catalyst, either Fe- or Cu-ZSM-5 are used, as they are also widely utilized in practical applications and they are well characterized from both chemical and engineering point of view, as well. As soot oxidation catalyst, CeO_2-PrO_2 was impregnated with potassium to tailor its reactivity towards the various components, as will be described later. In view of possible applications, a nominal content of 1.0 wt.% potassium was used, i.e. much lower than in our previous work [32].

2. Materials and methods

2.1 Catalysts preparation

Fe-ZSM-5 and Cu-ZSM-5 were used as SCR catalysts, since they are widely recognized as state-of-the-art catalyst and they have been characterized in previous works [10,23]. In a typical synthesis, 1.0 g H-

ZSM-5 (Alfa-Aesar) with SiO_2:Al_2O_3 ratio 23:1 and specific surface area of 425 m^2 g^{-1} was contacted with a 50.0 mM solution of iron(III) nitrate or copper(II) acetate to obtain Fe-ZSM-5 and Cu-ZSM-5, respectively. The suspension was stirred at room temperature for 24 h to allow ion exchange. After stirring, the slurry was separated by centrifugation and washed 4 times. The washed zeolites were dried for 12 hours at 120 °C and calcined at 700 °C for 5 h. The final Fe content in the Fe-ZSM-5 was 0.4 wt. % and the final Cu content in Cu-ZSM-5 was 4.1 wt. %, as determined by Inductively Coupled Plasma Atomic Emission Spectroscopy (ICP-AES) analyses. In the reactivity tests, Printex U (Degussa) soot was used. According to the supplier, the soot has an average particle size of 25 nm and a specific surface area of 88 m^2 g^{-1} indicating a highly porous sample. Printex U is considered as a model soot by scientific literature and it should be noted that it is generally less reactive that real diesel soot: as a consequence, the obtained results can be considered conservative [33].

The CeO_2-PrO_2 catalyst (hereafter referred to as CP) for the soot and selective NO oxidation was prepared by a hydrothermal synthesis procedure and characterized as detailed elsewhere [34]. Briefly, an equimolar solution of $Ce(NO_3)_3 \cdot 6H_2O$ and $Pr(NO_3)_3 \cdot H_2O$ was added drop wise to an 8.0 M NaOH solution under stirring. The obtained precipitate was aged for 1 hour and transferred into a Teflon autoclave. The crystallization was performed under hydrothermal conditions at 180 °C for 24 h. After cooling, the precipitate was centrifuged and washed several times until neutral pH was reached. The slurry was then dried for 12 hours at 120 °C and calcined at 700 °C for 5 h with a heating rate of 5 °C/min.

The K/CeO_2-PrO_2 sample (hereafter referred to as KCP) was prepared by wet impregnation with a 3 wt. % potassium carbonate nominal loading. The previously prepared CP sample was mixed to an appropriate amount of 0.03 M K_2CO_3 solution. The water was evaporated at 80 °C under constant stirring and the resulting powder was dried for 12 h at 100 °C and calcined for 3 h at 700 °C (heating rate = 5

°C/min). For the demonstration of ammonia over-oxidation, a Pt/Al_2O_3 catalyst with 5 wt. % Pt (Sigma-Aldrich) was used as reference catalyst for soot oxidation in the physical mixture.

2.2. Catalysts characterization

The XRD diffractograms were recorded on a X'Pert Philips PW3040 diffractometer equipped with a Pixel detector using a Cu Kα radiation in the 2θ range 20-80° degrees with 0.013° step size.

The specific surface area was determined by a Tristar II 3020 instrument (Micrometrics) by N_2 physisorption at -196 °C. Prior measurement, the catalyst was pretreated under vacuum at 200 °C for 2 h to remove water and other atmospheric contaminants. The reported values of specific surface area (S_{BET}) have been calculated according to the BET (Brunauer-Emmett-Teller) method.

The morphology and elemental composition of the catalysts were determined by Field Emission Scanning Electron Microscopy-Energy Dispersive X-ray Spectroscopy (FESEM-EDS) under high vacuum, using Zeiss MERLIN Gemini II equipped with EDS at 3 keV accelerating voltage and different magnifications.

Fourier Transform InfraRed (FT-IR) spectra were obtained with both the KCP and NO_x-saturated KCP catalyst to investigate surface species before and after NO_x saturation. For IR spectra measurement, the powder catalyst was pressed in a thin, self-supporting wafer, loaded inside a quartz cell equipped with (IR transparent) KBr windows and outgassed for 30 min at 100 °C in a vacuum frame (residual pressure below 10^{-3} mbar). IR spectra were collected at 2 cm^{-1} resolution on a BRUKER EQUINOX-66 spectrometer, equipped with a mercury cadmium telluride (MCT) cryodetector.

To characterize the relevant adsorption/desorption kinetics and the catalyst surface acid/base sites, NO_x temperature programmed desorption-oxidation (TPDO) and NH_3 temperature programmed desorption (TPD) were performed on both the CP and KCP catalysts by using the following experimental setup. Before the NO_x TPDO, the KCP catalyst was pre-saturated with 250 ppm NO and 250 ppm NO_2 at 250

°C. To observe the catalytic reactivity of the adsorbed NO_x with soot, NO_x was desorbed in the presence and absence of soot with a heating rate of 2 °C/min in the temperature range 200-800 °C. The sweep gas during desorption was 4 vol% O_2 in N_2 to avoid potential NO_x decomposition at high temperatures [32]. NH_3 adsorption and oxidation was performed in order to get insights into NH_3 reactivity, which is intimately related to SCR reactivity. Before NH_3 adsorption, the catalyst was pretreated at 400 °C to remove any adsorbed species (e.g. H_2O, CO_2) and saturated by flowing 1000 ppm NH_3 in N_2 at 50 °C. After adsorption and cooling down to room temperature, (adsorbed) NH_3 was desorbed by flowing inert N_2 gas and increasing temperature up to 600 °C with a 5 °C/min heating rate.

Impregnation with potassium did not significantly change the other physico-chemical characteristics of the CP catalyst, other detailed characterization on the same catalyst (X-ray Photoelectron Spectroscopy, Temperature Programmed Reduction) having been reported elsewhere [34].

2.3. Catalytic activity tests

Catalytic activity tests were run in a 10 mm internal diameter tubular glass reactor, heated by an isolated vertical tube furnace programmable with the desired heating rate. The investigated catalyst (or mixture of catalysts), pelletized and sieved to obtain particles below 250 μm, was placed in the reactor in order to obtain a fixed bed. A thermocouple was inserted on the top layer of the catalytic bed for continuous thermal measurements of the reaction temperature. The desired reaction gas mixtures were controlled by mass flow controllers. The typical gas concentrations used were 4 % O_2, 500 ppm NO_x ($NO+NO_2$) with different NO_2/NO_x ratios, 500 ppm NH_3 and balanced with N_2. The reaction species continuously monitored were NO, NO_2, CO_2, CO, NH_3 and N_2O by NDIR and UV analyzers with the appropriate filters (ABB AO2020 Uras and Limas). A bypass valve was installed before the reactor and the concentrations were monitored before and after passing through the catalytic bed.

Soot oxidation by O_2 was run by gently mixing 270 mg of the selected catalyst with 30 mg of soot with a spatula for 30 seconds to obtain a loose contact, whereas tight contact was achieved by ball-milling the catalyst-soot mixture for 15 minutes. The reaction was initiated at 200 °C with a 2°C/min heating rate and a 600 mL/min flow of a gas mixture containing 4 % O_2 in N_2.

NO_x-assisted soot oxidation was run with the same parameters, besides the addition of 500 ppm of NO in the gaseous reacting mixture. To compare the efficiency of NO_2 utilization for soot oxidation, NO oxidation was performed under the same conditions without soot and the NO_2/NO_x was compared.

NH_3 oxidation was also performed over CP and KCP catalysts in order to explain the observed SCR activities and interaction between the soot oxidation catalyst and the SCR catalyst. NH_3 was oxidized by flowing 600 mL/min of 500 ppm NH_3, 4% O_2 in N_2 over 270 mg of catalyst. As NO_x is a stronger oxidant than O_2 alone, NH_3 oxidation was also performed under the same reaction conditions as before in the presence of 500 ppm NO. The temperature was increased stepwise by increments of 40 °C and the reported values are obtained after stabilization in isothermal conditions.

The combined soot oxidation and NO_x SCR was conducted by flowing 600 mL/min of 4% O_2, 500 ppm NO_x and 500 ppm NH_3 in N_2 over 270 mg of catalyst with or without 30 mg of soot. Usually, standard SCR was conducted with the NO_2/NO_x ratio adjusted to 0 or, when specified, fast SCR was conducted with the NO_2/NO_x ratio set to 0.5. The used catalysts were Fe-ZSM-5, Cu-ZSM-5, CP and KCP individually, as well as their physical mixtures.

In order to investigate likely interactions among the processes of soot oxidation, NO oxidation and SCR reactions, the developed KCP soot oxidation catalyst was physically mixed with the Fe-ZSM-5 and Cu-ZSM-5 SCR catalyst in different mass ratios. Different reaction conditions and configurations were also examined, to demonstrate that the proposed integrated soot oxidation-SCR system is not limited only to specific types of SCR catalysts and reaction conditions but can be extended and applied to general cases. Different reaction conditions and physical mixtures were used and the system performance in the soot

and NO_x abatement was compared with the results obtained for the individual catalysts. Combined soot oxidation and standard and fast SCR were conducted always keeping a total catalyst mass of 270 mg with 30 mg of soot and a gas flow of 600 mL/min, maintaining the *w/f* always constant. In the physical mixture, the combined soot oxidation-SCR reaction, the inlet gas concentration was 500 ppm NO, 500 ppm NH_3, 4 % O_2 in N_2. A temperature increase of 2 °C/min was used starting at 200 °C, and, after burning the soot, the NO_x conversion was observed under the same conditions without soot to quantify the interaction of soot and the SCR reaction. When a significant difference (> 2 %) of NO_x conversion was observed, both in the presence and absence of soot, the deviation was marked on the figures with dots. To quantify the interaction between the two different SCR and soot oxidation catalysts, they were loosely mixed in different mass ratios keeping the total mass constant at 270 mg in all the experiments. With the physical mixture with Fe-ZSM-5, the following cases were considered:

1. Case I: Fe-ZSM-5:KCP:soot mixed in mass ratio 6:3:1 respectively.

2. Case II: Fe-ZSM-5:KCP:soot mixed in mass ratio 3:6:1.

3. Case III: Fe-ZSM-5:KCP:soot mixed in mass ratio 4.5:4.5:1.

4. Case IV: Fe-ZSM-5:KCP:soot mixed in mass ratio 6:3:1 with NO_2/NO_x ratio 0.5 (fast SCR).

For the low temperature applications, soot integration was examined over Cu-ZSM-5. In this case, as will be shown later, low NO_2 concentration is not limiting the SCR reaction as much as on Fe-ZSM-5 [10,12] and lower amount of the soot oxidation catalyst is preferable. The following physical mixtures in loose contact were examined:

1. Case I: Cu-ZSM-5:KCP:soot mixed in mass ratio 6:3:1.

2. Case II: Cu-ZSM-5:KCP:soot mixed in mass ratio 7.6:1.6:1.

3. Case III: Cu-ZSM-5:KCP:soot mixed in mass ratio 7.6:1.6:1 with NO_2/NO_x ratio 0.5.

4. Case IV: To demonstrate the effect of the reductant over-oxidation, the Cu-ZSM-5 was mixed with Pt/Al_2O_3 and soot in mass ratio 7.6:1.6:1.

The sensitivity of CP and KCP towards sulphur poisoning was tested as NO oxidation catalysts are typically deactivated in the presence of SO_2. The deactivation tests were performed at a constant temperature of 350 °C under the same reaction conditions of NO oxidation tests. After reaching a stable NO_x concentration, 60 ppm of SO_2 was introduced in the reaction stream and the decrease of the NO_2/NO_x ratio over time was observed. The thermal stability and recyclability of KCP was tested by cyclic soot oxidation in O_2 and a total of five repetitions was performed.

3. Results and discussion

3.1. Characterization results

No relevant differences in the XRD patterns of both KCP and CP in Figure S1 were observed, in agreement with the low potassium loading, which is likely also very dispersed at the surface. The characteristic diffraction peaks of CP correspond to the fluorite cubic ceria structure, indicating that Ce and Pr form a solid solution without potassium insertion in the crystalline lattice. The crystallite size, as calculated according to the Scherrer equation, was ca. 30 nm for both CP and KCP.

The FE-SEM micrographs of CP and KCP (Figure S2) show that KCP particles are slightly larger and more rounded than CP particles, indicating a uniform deposition of K_2CO_3. The BET surface area of KCP is somewhat lower than that of CP (9.0 and 24 m^2/g, respectively) meaning that some of the deposited K_2CO_3 was likely plugging the porous channels. The observed rod structure, instead, was the result of the hydrothermal synthesis method and it was shown to induce superior soot oxidation activity [34].

The FE-SEM images of the physical mixtures of KCP with either Fe-ZSM-5 or Cu-ZSM-5 are shown in Figure 1, where the micrographs of the samples recovered after 2 tests are reported. The different zeolite and KCP particles occurred separately at significant distance (or the order of μm), indicating that coalescence (or melting) phenomena did not occur (or occurred to a limited extent) even after the

catalysts were subjected to high temperature (700 °C) during the combined soot oxidation-SCR reaction. The provided evidence demonstrates that the two reactions and the related phenomena occurring on the two catalysts in loose contact are likely occurring separately and no direct spillover of the reaction species is occuring. In contrast, when two catalysts are in tight contact, direct transport of the intermediates is possible, as shown by [26–31].

In Figure 2, the NO_x TPDO curves on the samples CP and KCP are shown. In the absence of soot, the adsorbed nitrates on KCP are stable and desorption starts only above 450 °C, finishing with complete depletion above 750 °C. In contrast, when the NO_x-saturated KCP is mixed with soot in loose contact, the NO_x present on the catalyst is destabilized, as oxygen is transferred to the soot and desorbed at significantly lower temperatures. Concurrently, NO_2 is reduced to NO and soot oxidation is enhanced (see Figure 2). NO is released yet at 350 °C, however a fraction of NO_x remains adsorbed and is released at high temperatures (> 600 °C). The total amount of released NO_x was 0.74 mmol/g both in the presence and absence of soot, meaning that in oxidizing atmosphere NO_2 is reduced to NO and not to N_2. This proves that potassium is catalytically active not only towards the soot-O_2 reaction, but also towards the soot-NO_2-O_2 reaction. It can be hypothesized that soot acts as an oxygen acceptor and destabilizes the adsorbed NO_2, however the exact mechanism and reaction intermediates are still largely unknown [35–37]. Due to the lack of alkali metal, CP presented a much lower NO_x adsorption capacity and a very heterogeneous surface. Although several adsorption sites were observed, the strength of adsorption was much lower than in the presence of potassium at the surface, and NO_x was released at much lower temperatures as compared to KCP. No notable difference in the desorption profile was observed when soot was mixed with the CP sample, meaning that it is not active for the soot-NO_2-O_2 reaction, but NO_2 is desorbed and reacts in gas phase.

In order to confirm the chemical interaction of NO_x with the catalyst surface, IR spectra were taken of the KCP catalyst before and after reaction (Figure S3): as expected, before reaction the IR spectrum is

dominated by the absorption bands due to carbonate ions in the 1700 – 1200 cm^{-1} range, whereas saturation with NO$_x$ led to the appearance of broad bands between 1300 and 1450 cm^{-1}, ascribed to the symmetric stretching mode of nitrate ions. Bidentate chelating nitrates were also evidenced by the weak band between 1000-1100 cm^{-1} and the shoulder between 1450-1600 cm^{-1}. Nitrosyl species should absorb at 1750 cm^{-1}, however here the N=O stretching mode would overlap to the vibration of nitrate and cannot be identified unambiguously in the reported IR spectrum. The sharp peak at 1750 cm^{-1} is more likely due to nitrate species, also by considering the intensity of the 1300-1400 cm^{-1} bands [38,39].

In Figure 3, the ammonia TPD curves of the CP and KCP samples are shown. The CP sample showed a limited amount of acid sites that can adsorb and activate ammonia molecules, whereas on KCP no ammonia adsorption (or desorption) was observed. Gaseous ammonia adsorption and activation occurs on both Lewis and Brønsted acid sites, producing various intermediates, acid sites being crucial for NH$_3$-mediated SCR [40,41]. Here, the strategy to avoid ammonia over-oxidation involved the addition of potassium, as it effectively poisons (Brønsted) acid sites (by likely substituting surface protons), which are responsible for the activation of NH$_3$. For similar reasons, potassium is used as a promoter on catalysts for ammonia synthesis, where it has been shown that favours ammonia desorption [41]. By tailoring the surface properties and acidity, the NH$_3$ oxidation can be prevented, without negative effects on the soot oxidation. The amount of ammonia molecules adsorbed on CP acid sites was 3.65 µmol/g$_{cat}$, (as calculated from integration of the desorption curve in Figure 3), whereas no sizeable adsorption of ammonia was measured on the KCP sample, notwithstanding the presence of 1.0 wt. % K (nominal content). If all the potassium sites were available as Lewis sites, the amount of adsorbed ammonia would be 250 µmol/g$_{cat}$, but likely potassium ions are poorly accessible and/or too large (i.e. with a too small charge/radius ratio) to effectively act as Lewis acids sites towards ammonia molecules. This is an important point, since, as reported in the literature [26–31], over-oxidation of the reductant (here, NH$_3$) would be detrimental for SCR reaction (*vide infra*).

3.2. Catalytic activity of individual catalysts

As described in equations R1-5, the oxidation of ammonia is competitive with the SCR reactions (both standard and fast) and the relative amount of NH_3 used as a NO_x reductant or wasted in the oxidation is crucial for the SCR performance. The addition of potassium poisoned the acid sites on the soot oxidation catalyst and, correspondingly, the NH_3 oxidation activity decreased significantly (see Figure 3 and 4). The NH_3 oxidation was delayed by more than 150 degrees in both O_2 and O_2 + NO_x reaction mixtures. While on CP almost full NH_3 conversion was observed at 400 °C, on KCP the NH_3 oxidation just initiated at that temperature and full conversion was reached only above 550 °C. In the presence of 500 ppm NO, NH_3 oxidation started earlier, partially also due to the occurrence of some NO_x SCR, however full conversion was reached approximately at the same temperature as without NO_x.

The O_2-mediated soot oxidation on both CP and KCP improved significantly with respect to the non-catalyzed soot oxidation, as illustrated in Figure 5. The CP sample lowered by 50 °C the soot oxidation temperature and the addition of 3 wt. % potassium carbonate further lowered it by 100 °C. However, the most significant improvement was observed in the presence of NO, as both CP and KCP can oxidize NO to NO_2. In the presence of NO_x, soot oxidation proceeded at much lower temperatures in comparison with O_2 alone. The soot oxidation rates were similar over CP and KCP, and soot oxidation started at a temperature as low as 250 °C, reaching a maximum already at 450 °C. KCP showed a double peak, as dynamic NO_x adsorption-reaction due to potassium played a significant role in the reaction: when NO was re-oxidized and desorbed, a sudden increase in the soot oxidation rate occurred and a smaller second peak appeared. When tight contact was adopted between soot and the KCP catalyst, the curve of soot oxidation in the presence of only O_2 shifted by 50 degrees to lower temperatures, while in the presence of the O_2+NO_x mixture, the soot oxidation exhibited a steep increase and the soot was oxidized in a shorter period with respect to the loose contact. The peak of soot oxidation was accompanied by a rapid

increase in NO concentration, suggesting the dominant contribution of R7 and the enhanced contribution of surface nitrates to soot oxidation.

When the KCP catalyst was saturated with NO_x before the reaction, its performance in soot oxidation without NO_x in the inlet gas was as good as with NO_x in the reaction mixture. The nitrates stored at the catalyst surface in the presence of potassium took place to the reaction (see NO_x TPDO in Figure 2), significantly enhancing the soot oxidation. The stored NO_2 at the catalyst surface in the presence of potassium could participate in the soot oxidation and it was released as NO starting at 350 °C. However, the improvement was only temporary, and it could be replicated only if the catalyst was saturated with NO_x again before the oxidation.

On both the CP and KCP samples, the NO oxidation started at 250 °C and reached a maximum NO_2/NO_x ratio of ca. 0.45 at 350 °C (Figure 6). No significant difference in the NO oxidation activity was observed between CP and KCP, despite the much lower surface area of KCP (24 and 9 m^2/g, respectively). During the NO_x-assisted soot oxidation, the NO_2/NO_x ratio was significantly lowered. In both the KCP and CP catalysts, the ratio was lowered by almost 0.2 as the NO_2 was being consumed for soot oxidation and producing NO, according to equation R7. This is even more obvious on the KCP, as the adsorption/desorption dynamics during soot oxidation produced high variations in the NO_x. This result is relevant for the SCR, as the presence of soot can somewhat lower the NO_2/NO_x ratio and, in some cases, have negative effect on the NO_x conversion as it is lower than 0.5. Only when the NO_2/NO_x ratio is higher than 0.5, the presence of soot has a positive effect on NO_x conversion as it consumes the NO_2 and adjusts the ratio to the fast SCR regime [11,18].

As SCR catalysts, Fe-ZSM-5 and Cu-ZSM-5 were used as they have superior stability, high NO_x conversion and selectivity and wide operational temperature range. For these reasons, in the majority of practical applications, metal-exchanged zeolites are used as SCR catalysts [10,19,42]. As shown in Figure 7, the Fe-exchanged zeolite had superior performance in the high temperature region, while the

Cu exchanged one in the low temperature region. For this reason, Fe zeolites are mainly used for the aftertreatment in HDD and Cu zeolites for LDD applications [10,19,42]. Fe-ZSM-5 is much more sensitive to excessive ammonia adsorption and coverage, and, accordingly, there is a large difference between the fast and standard SCR. It is generally acknowledged that Fe zeolites are more sensitive to NO_2/NO_x ratio than their Cu counterparts (Figure 7) [10,43]. With the fast SCR gas mixture, high NO_x conversions are reached with both catalysts, even at the high flow rates used in this study. On the other hand, the standard SCR is limited at low temperatures for Fe-ZSM-5. At higher temperatures (>400 ˚C), Fe-ZSM-5 can oxidize NO and the ammonia coverage is lower and NO_x conversion rises. In contrast, Cu-ZSM-5 is not as sensitive to the NO_2/NO_x ratio at lower temperature and, accordingly, there is a much smaller difference between the fast and standard SCR. Due to over-oxidation of ammonia, a steady decrease in NO_x conversion initiates already at 300 ˚C. The selectivity was much better on Fe-ZSM-5 as compared to Cu-ZSM-5 (Figure 11), in accordance with the literature [43]. While on the Fe zeolite very little N_2O was observed, and selectivity was always above 95%, over Cu zeolite, at its maximum, 50 ppm N_2O was produced. The selection between Fe- or Cu-zeolites for the SCRoF application depends on a variety of factors, such as the expected working exhaust temperature, the DOC performance and the NO_2/NO_x ratio, the stability requirements, etc.

The soot oxidation catalysts, CP and KCP, individually presented negligible SCR activity in the range 250-350 ˚C, as the NO_x conversion never exceeded 15%. Above 350 ˚C, the NOx conversion was "negative" over CP and KCP as ammonia was non-selectively oxidized to NO. From this, we can infer that any improvement observed due to the mixing of the soot oxidation with an SCR catalyst is due to phenomena other than simply their linear combination.

The biggest issue of the SCRoF is that the soot oxidation is inhibited as the NO_2 is consumed in the much faster SCR reaction, leaving none NO_2 for soot oxidation. This was demonstrated in detail in several reports [11,13,19,44] and, in Figure 8, for both the Cu- and Fe-ZSM-5 catalysts. Without dosing NH_3,

and hence without the occurrence of the SCR reaction, the soot oxidation initiates at a temperature as low as 300 ˚C and reaches a plateau due to limited availability of NO_2. However, with the addition of NH_3 in the reaction gas, the NO_x is converted by the much faster SCR reaction, and the soot oxidation profiles are practically the same as for the non-catalytic soot oxidation. In the SCRoF system, the main oxidant available is O_2 and the contribution of NO_2 to the oxidation of soot is inhibited by the kinetically much faster SCR reaction. For this reason, very high regeneration temperatures are necessary, which can damage the filter or the catalyst. The only conditions where NO_2 could participate in the soot oxidation on SCRoF would be if the soot-NO_2-O_2 reaction was catalyzed and significant amount of NO_2 was present (i.e. NO_2/NO_x ratio higher than 0.5). This is of course not practical, as the NO_x conversion should not be compromised on the SCRoF systems.

3.3. Catalytic activity of the dual components system

Figures 9 and 10 show the catalytic activities for NO_x reduction and soot oxidation of the physical mixtures of KCP and Fe and Cu zeolites in different mass fractions. Both standard and fast SCR were measured, coupled with soot oxidation and benchmarked to the cases when Fe and Cu zeolites were used without soot oxidation catalysts, while the soot oxidation performance was compared to that of soot oxidation on KCP in O_2 and O_2 + NO_x.

For the system based on Fe-zeolite, the following Fe-ZSM-5:KCP ratios were tested in standard SCR conditions: 1:2, 1:1 and 2:1, as well as the optimal 2:1 ratio mixture in fast SCR conditions. From the NO_x-SCR viewpoint, the worst results were obtained when the least amount of the Fe-ZSM-5 catalyst was used (1:2 ratio), as there was not enough catalyst to perform NO_x reduction. Furthermore, above 500 ˚C, a sharp decline in NO_x conversion occurred, as ammonia started to be oxidized. Due to low NO_x conversion, there was plenty of NO_2 available and the soot oxidation profile was shifted to the lowest temperature amongst the three mixtures.

Regarding NO_x conversion, the mixture with 2:1 mass ratio showed the best performance. At low temperatures, the same performance was observed as with 270 mg of Fe-ZSM-5, however above 300 ˚C the NO_x conversion significantly increased with the physical mixture, presenting nearly 20% improved conversion in a wide temperature range as compared to Fe-ZSM-5 alone. This can be explained with the partial transformation of the NO_x reaction pathway from standard to fast SCR. As can be seen in Figure 7, significant NO oxidation initiates at 300 ˚C on the KCP catalyst and the largest difference was observed at 450 ˚C, when NO oxidation is not kinetically limited. As lower amount of KCP was used in the mixture, ammonia oxidation was not pronounced and, as compared to Fe-ZSM-5 alone, slightly lower SCR performance was observed only above 600 ˚C due to ammonia over-oxidation. In this physical mixture, the soot oxidation was also significantly improved, as compared to Fe-ZSM-5 alone. However, since high NO_x conversions were achieved in the combined SCR and soot oxidation reactions, NO_2 could not participate significantly in the soot oxidation and the CO_x profile was more similar to the one obtained during soot oxidation on KCP with only O_2 (Figures 9 and 10). These results are in agreement with previous studies [11,13–19], which demonstrated that, in the simultaneous presence of soot oxidation and NO_x SCR reactions, NO_2 reduction is kinetically much faster and its contribution to soot oxidation is inhibited. Soot oxidation started at lower temperatures, indicating at least a partial contribution of NO_2 to the process. It also took more time to reach complete soot oxidation, due to a less effective contact bewteen KCP and soot, as the SCR catalyst presented a physical barrier, indicating that a portion of the soot was non-catalytically oxidized.

When the KCP and Fe-ZSM-5 were mixed in equal amounts, the NO_x SCR performance was better than with Fe-ZSM-5 alone, however worse than the 2:1 mass ratio mixture. At higher relative amount of the soot oxidation catalyst, NH_3 oxidation was more pronounced and NO_x conversion decreased significantly above 550 ˚C. For the same reason, soot oxidation was slightly better than in the previous case, however it still approached the soot oxidation curve of the test carried out with only O_2 over KCP. By comparing

the three mixtures, only with the 1:1 mass ratio a significant difference in the NO_x conversion (~10%) in the presence and absence of soot was observed in the initial temperature range of soot oxidation. As KCP catalyzed the NO_2-soot oxidation (see Figure 2 and 6), it also decreased the NO_2/NO_x ratio in the presence of soot consequently lowering the contribution of fast SCR. In the other two cases, this phenomenon was not observed, since the relative amount of Fe-ZSM-5 was high, thus the NO_2 was depleted because of the fast SCR and there was not enough KCP for NO_2-soot reaction to proceed. In contrast, when the relative Fe-ZSM-5 content was low, the NO oxidation could proceed and plenty of NO_2 was produced, hence SCR was not limited by NO_2-soot reaction.

With the inlet NO_2/NO_x ratio adjusted to 0.5, the combined soot oxidation and fast SCR was performed for the mixture having a Fe-ZSM-5:KCP ratio of 2:1. Due to the lower amount of the SCR catalyst (180 mg vs. 270 mg) in the catalytic system, NO_x conversion was much lower in the low temperature range (c.a. 20% less) as compared to Fe-ZSM-5 alone. However, as the temperature increased above 300 ˚C, it approached the profile of Fe-ZSM-5 alone. In terms of NO_x conversion, no improvement was observed with the physical mixture, since SCR was already in the fast regime and no transformation of standard-to-fast SCR occurred. Soot oxidation was slightly improved in the fast SCR regime, as compared to the standard SCR, under the same conditions, most likely due to the improved NO oxidation and slight NO_2 contribution at higher temperature. The same principle applies, however, as in the previous case, i.e. NO_2 did not contribute significantly to soot oxidation due to the faster and simultaneous SCR reactions.

To extend and generalize the concept of simultaneous improvement of NO_x and soot removal, the tests were repeated with the Cu-ZSM-5 catalyst. Cu-zeolites are, in general, less sensitive to the NO_2/NO_x ratio and they have better NO_x performance at low temperatures. This, however, is achieved in spite of ammonia over-oxidation at higher temperatures and higher N_2O production compared to Fe zeolites [43]. In Figure 10, the behavior of a soot oxidation catalyst mixed with Cu-ZSM-5 is shown. As SCR on Cu-ZSM-5 is not as sensitive as Fe-ZSM-5 to the NO_2/NO_x ratio, a lower amount of the soot oxidation

catalyst was used in the physical mixture. Below 300 ˚C, as there was no significant NO oxidation on KCP, the conversion decreased proportionally to the amount of Cu-ZSM-5 present. However, also a small improvement (~5%) in NO_x conversion occurred in the 300-400 ˚C range for the Cu-ZSM-5:KCP 4.5:1 mixture, when NO oxidation became significant.

Fast SCR was also performed for the physical mixture having a Cu-ZSM-5:KCP ratio of 4.5:1. Below 400 ˚C, the performance was the same as with Cu-ZSM-5 alone, whereas at higher temperatures the NO_x conversion decreased by ~15% as ammonia was non-selectively oxidized. From this, it can be inferred that for Cu-ZSM-5 only small improvements are possible in exploiting the pathway of transformation of the reaction system from standard to fast SCR, and they are more sensitive to ammonia over-oxidation as compared to Fe-zeolites.

Soot oxidation was significantly improved in the physical mixture as compared to Cu-ZSM-5 alone. As with the Fe-ZSM-5 catalyst, the soot oxidation in the mixture was more similar to the soot oxidation in the presence of O_2 catalyzed by KCP. It is important to note that, while the peak of maximum soot oxidation almost matched, soot oxidation started at a lower temperature (by ca. 50 degrees), indicating at least the partial involvement of NO_2. Since the SCR catalyst acted as a physical barrier to the soot oxidation catalyst, soot oxidation needed more time and higher temperatures to be complete, implying that at least a portion of the soot was non-catalytically burned. From this, it can be inferred that washcoating of the monolith with a soot oxidation catalyst is an important parameter and should be done on the inlet side so as to maximize the catalyst-soot contact. The CO emission in the case of the physical mixture was also significantly lowered and remained always under 100 ppm (Figure S4), since higher selectivity towards CO_2 was achieved in the catalytic soot oxidation. While in the case of the Cu-ZSM-5 catalyst alone the selectivity towards CO was as high as 30%, with all the physical mixtures it remained below 5%.

The N_2O production with the physical mixture was very similar to that obtained with the SCR catalyst alone, so only those for the optimal mixture are shown in Figure 11. Cu-ZSM-5 had much higher N_2O production than Fe-ZSM-5 and N_2O concentration reached almost 50 ppm in the fast SCR.

To demonstrate the effect of ammonia oxidation on the SCR reactions, Cu-ZSM-5 was mixed with Pt/Al_2O_3 in 4.5:1 ratio and simultaneous SCR and soot oxidation reactions were performed. As shown in Figures 10a and 11, NO_x conversion quickly decreased and, due to the non-selective oxidation of ammonia, almost 250 ppm of N_2O was present in the outlet. Such a result highlights the importance of the fact that the soot and the NO oxidation catalysts must not be oxidative towards ammonia, otherwise they would decrease the amount of the reductant available for NO_x SCR, producing undesired reaction products.

3.4. Stability of the soot oxidation catalyst

SO_2 is a known poison for NO oxidation catalysts, as it can adsorb on the active sites and form stable sulfates, thereby inhibiting NO oxidation. When exposed to SO_2, CP underwent severe deactivation, and complete deactivation was observed after ca. 150 min (Figure S5A). On the other hand, with KCP the NO_2/NO_x ratio decreased only by ca. 15% after 150 min and the catalyst retained significant NO oxidation activity even after 6 hours of exposure, indicating that the adsorbed nitrates were very stable, avoiding the formation of sulphates.

The thermal stability of KCP was demonstrated by repeated soot oxidation tests (Figure S5B). As soot oxidation catalyst, potassium is known to have low stability under certain conditions [32,45], however several methods were proposed for its stabilization [46,47]. The stability of potassium in KCP was ensured by low loading and high calcination temperature, which enabled strong anchoring on the support and consistent performance. As shown in Figure S5B, after 5 repeated soot oxidation cycles the soot

oxidation temperature decreased only by 15 ˚C, confirming the thermal stability of KCP during soot oxidation.

4. Conclusions

The soot oxidation on SCRoF was successfully enhanced to address the problem of soot accumulation by the combination of a common SCR catalyst and a soot and NO oxidation catalyst. The soot oxidation on the single component (either Cu-ZSM-5 or Fe-ZSM-5) was significantly inhibited by NO_2 consumption in the kinetically much faster SCR reaction and temperatures above 600 °C were required to oxidize all the soot. However, by mixing a soot oxidation catalyst and a common SCR catalyst, the temperature of soot oxidation was lowered by more than 150 degrees, while maintaining high NO_x conversion. In the physical mixture, the soot was oxidized mainly by O_2, since the contribution of NO_2 was limited because it reacted in the (kinetically much faster) SCR reaction. Avoiding ammonia oxidation by the soot oxidation catalyst was crucial, as the consumption of the reductant inhibited the performance of the SCR reaction. This was achieved by targeted poisoning of the acid sites on the soot oxidation catalyst through its impregnation with only 3.0 wt. % potassium carbonate.

The K/CeO_2-PrO_2 soot oxidation catalyst was also selectively active towards NO oxidation, simultaneously improving NO_x conversion by transforming the SCR reaction pathway from standard to fast SCR. As SCR catalyst, Cu-ZSM-5 offered better performance at low temperature and Fe-ZSM-5 in the higher temperature range, while in fast SCR regime both catalysts offered high activity in a wide temperature range. By varying the relative amounts of the soot oxidation and SCR catalysts, several relevant phenomena were observed. In the physical mixture, for the optimal Fe-ZSM-5:KCP ratio of 2:1, almost 20 % improvement in NO_x conversion was observed with respect to the same amount of Fe-ZSM-5 alone (1:0 "ratio"). In contrast, since Cu-ZSM-5 was not as much sensitive to the NO_2/NO_x inlet ratio, the improvement in the physical mixture was limited (ca. 5%) and observed only above 300 °C. Cu-

ZSM-5 was however more sensitive to ammonia oxidation and thereby the optimal ratio of the Cu-ZSM-5:KCP was 4.5:1, i.e. much higher than in the case of Fe-ZSM-5. A lower SCR catalyst:KCP ratio was beneficial for the soot oxidation however it lowered the NO_x conversion as less SCR catalyst was available.

Finally, it should be emphasized that the tests were run in a laboratory setup, with the main aim of providing a detailed study on the interaction between a soot oxidation catalyst and a SCR catalyst. Besides chemical interactions, on a real monolith other important parameters should also be taken into account: fluid-dynamics and pressure drop are important variables, as well as catalyst loading and distribution in the monolith. Furthermore, the effect of the contact between soot and oxidation catalyst should be carefully evaluated, as different contact length with the filtered soot cake can limit the effective range of action of the catalyst.

References

[1]   M. Schejbal, J. Štěpánek, M. Marek, P. Kočí, M. Kubíček, Fuel 89 (2010) 2365–2375.

[2]   M.D. Tomić, L.D. Savin, R.D. Mićić, M.D. Simikić, T.F. Furman, Therm. Sci. 17 (2013) 263–278.

[3]   S.M. Platt, I. El Haddad, S.M. Pieber, A.A. Zardini, R. Suarez-Bertoa, M. Clairotte, K.R. Daellenbach, R.J. Huang, J.G. Slowik, S. Hellebust, B. Temime-Roussel, N. Marchand, J. De Gouw, J.L. Jimenez, P.L. Hayes, A.L. Robinson, U. Baltensperger, C. Astorga, A.S.H. Prévôt,

Sci. Rep. 7 (2017) 4926.

[4]   C.L. Myung, W. Jang, S. Kwon, J. Ko, D. Jin, S. Park, Energy 132 (2017) 356–369.

[5]   N. Hooftman, M. Messagie, J. Van Mierlo, T. Coosemans, Renew. Sustain. Energy Rev. 86 (2018) 1–21.

[6]   T.R. Dallmann, R.A. Harley, T.W. Kirchstetter, Environ. Sci. Technol. 45 (2011) 10773–10779.

[7]   T.R. Dallmann, S.J. Demartini, T.W. Kirchstetter, S.C. Herndon, T.B. Onasch, E.C. Wood, R.A. Harley, Environ. Sci. Technol. 46 (2012) 8511–8518.

[8]   D. Fino, S. Bensaid, M. Piumetti, N. Russo, Appl. Catal. A Gen. 509 (2016) 75–96.

[9]   G.J. Bartley, in: SAE Tech. Pap., 2015.

[10]   K. Kamasamudram, N. Currier, T. Szailer, A. Yezerets, SAE Int. J. Fuels Lubr. 3 (2010) 664–672.

[11]   K.G. Rappé, Ind. Eng. Chem. Res. 53 (2014) 17547–17557.

[12]   P.S. Metkar, M.P. Harold, V. Balakotaiah, Chem. Eng. Sci. 87 (2013) 51–66.

[13]   S. Bensaid, V. Balakotaiah, D. Luss, AIChE J. 63 (2017) 238–248.

[14]   F. Marchitti, I. Nova, E. Tronconi, Catal. Today 267 (2016) 110–118.

[15]   T. Wolff, R. Deinlein, H. Christensen, L. Larsen, SAE Int. J. Mater. Manuf. 7 (2014).

[16]   A.Y. Stakheev, G.N. Baeva, G.O. Bragina, N.S. Teleguina, A.L. Kustov, M. Grill, J.R. Thøgersen, in: Top. Catal., 2013, pp. 427–433.

[17]   S.Y. Park, K. Narayanaswamy, S.J. Schmieg, C.J. Rutland, Ind. Eng. Chem. Res. 51 (2012) 15582–15592.

[18]   D. Karamitros, G. Koltsakis, Chem. Eng. Sci. 173 (2017) 514–524.

[19]   W. Tang, D. Youngren, M. SantaMaria, S. Kumar, SAE Int. J. Engines 6 (2013) 862–872.

[20]   A. Sultana, M. Sasaki, K. Suzuki, H. Hamada, Appl. Catal. A Gen. 466 (2013) 179–184.

[21]   Z. Liu, J. Hao, L. Fu, T. Zhu, J. Li, X. Cui, Chem. Eng. Technol. 27 (2004) 77–79.

[22]   Y.K. Hong, D.W. Lee, Y.C. Ko, L. Yinghua, H.S. Han, K.Y. Lee, Catal. Letters 136 (2010) 106–115.

[23]   P.S. Metkar, M.P. Harold, V. Balakotaiah, Appl. Catal. B Environ. 111–112 (2012) 67–80.

[24]   T. Wittka, B. Holderbaum, P. Dittmann, S. Pischinger, Emiss. Control Sci. Technol. 1 (2015) 167–182.

[25]   M. Václavík, P. Kočí, V. Novák, D. Thompsett, Chem. Eng. J. 329 (2017) 128–134.

[26]   M. Misono, Y. Hirao, C. Yokoyama, Catal. Today 38 (1997) 157–162.

[27]   A.I. Mytareva, D.A. Bokarev, G.N. Baeva, D.S. Krivoruchenko, A.Y. Belyankin, A.Y. Stakheev, Pet. Chem. 56 (2016) 211–216.

[28]   A.I. Mytareva, D.A. Bokarev, G.N. Baeva, A.Y. Belyankin, A.Y. Stakheev, Top. Catal. 62 (2019) 192–197.

[29]   D.S. Krivoruchenko, N.S. Telegina, D.A. Bokarev, A.Y. Stakheev, Kinet. Catal. 56 (2015) 741–746.

[30]   M. Salazar, R. Becker, W. Grünert, Appl. Catal. B Environ. 165 (2015) 316–327.

[31]   M. Salazar, S. Hoffmann, O.P. Tkachenko, R. Becker, W. Grünert, Appl. Catal. B Environ. 182 (2016) 213–219.

[32]   F. Martinovic, T. Andana, F.A. Deorsola, S. Bensaid, R. Pirone, Catal. Letters 150 (2020) 573–585.

[33]   I. Atribak, A. Bueno-López, A. García-García, Combust. Flame 157 (2010) 2086–2094.

[34]   T. Andana, M. Piumetti, S. Bensaid, L. Veyre, C. Thieuleux, N. Russo, D. Fino, E.A. Quadrelli, R. Pirone, Appl. Catal. B Environ. 226 (2018) 147–161.

[35]   L. Castoldi, N. Artioli, R. Matarrese, L. Lietti, P. Forzatti, in: Catal. Today, 2010, pp. 384–389.

[36]   B.S. Sánchez, C.A. Querini, E.E. Miró, Appl. Catal. A Gen. 392 (2011) 158–165.

[37]   Q. Li, X. Wang, Y. Xin, Z. Zhang, Y. Zhang, C. Hao, M. Meng, L. Zheng, L. Zheng, Sci. Rep. 4 (2015) 4725.

[38]   I.S. Pieta, M. García-Diéguez, C. Herrera, M.A. Larrubia, L.J. Alemany, J. Catal. 270 (2010) 256–267.

[39]   R. Matarrese, L. Lietti, L. Castoldi, G. Busca, P. Forzatti, in: Top. Catal., 2013, pp. 477–482.

[40]   Y. Peng, J. Li, X. Huang, X. Li, W. Su, X. Sun, D. Wang, J. Hao, Environ. Sci. Technol. 48 (2014) 4515–4520.

[41]   K. ichi Tanaka, Dynamic Chemical Processes on Solid Surfaces: Chemical Reactions and Catalysis, 2017.

[42]   W. Tang, B. Chen, K. Hallstrom, A. Wille, SAE Int. J. Engines 9 (2016).

[43]   D. Zhang, R.T. Yang, Energy and Fuels 32 (2018) 2170–2182.

[44]   O. Mihai, S. Tamm, M. Stenfeldt, L. Olsson, Philos. Trans. R. Soc. A Math. Phys. Eng. Sci. 374 (2016) 20150086.

[45] R. Matarrese, E. Aneggi, L. Castoldi, J. Llorca, A. Trovarelli, L. Lietti, Catal. Today 267 (2016) 119–129.

[46] R. Kimura, J. Wakabayashi, S.P. Elangovan, M. Ogura, T. Okubo, J. Am. Chem. Soc. 130 (2008) 12844–12845.

[47] M. Ogura, R. Kimura, H. Ushiyama, F. Nikaido, K. Yamashita, T. Okubo, ChemCatChem 6 (2014) 479–484.

List of captions

Figure captions

Figure 1. FE-SEM images of the physical mixture of KCP and Cu-ZSM-5and Fe-ZSM-5 zeolites after reaction.

Figure 2. NO_x TPDO on the CP and KCP samples with and without soot.

Figure 3. Ammonia TPD over the CP and KCP samples.

Figure 4. Ammonia oxidation over CP and KCP catalysts. Reaction conditions: 500 ppm NH_3, 4% O_2 in N_2; *w/f* 27 g_{cat}·s /L. The dashed line case also contained 500 ppm NO_x.

Figure 5. Soot oxidation and NO_x assisted Oxidation on CP and KCP. Reaction conditions: 4% O_2 in N_2 and 500 ppm NO when indicated, *w/f* 27 g_{cat}·s/L, catalyst: soot mass ratio 9:1 in loose contact.

Figure 6. NO_2/NO_x ratio during NO oxidation and NO_x assisted soot oxidation. Reaction conditions: 500 ppm NO. 4% O_2 in N_2 and when indicated soot is present, *w/f* 27 g_{cat}·s/L, catalyst: soot mass ratio 9:1 in loose contact.

Figure 7. SCR activity of individual catalysts Fe and Cu-ZSM-5, CP and KCP. Reaction conditions: 500 ppm NO_x, 500 ppm NH_3, 4% O_2 in N_2; $NO_2/NO_x = 0$ for Standard SCR and 0.5 for Fast SCR; *w/f* 27 g_{cat}·s/L; catalyst: soot mass ratio 9:1 in loose contact; 2 ˚C/min heating rate.

Figure 8. Inhibition of soot oxidation by SCR reaction on Cu-ZSM-5 and Fe-ZSM-5. Reaction conditions: 4% O_2 in N_2 and 500 ppm NO_x, NO_2/NO_x ratio 0.5, 500 ppm NH_3 added when indicated; *w/f* 27 $g_{cat}\cdot$s/L; catalyst: soot mass ratio 9:1 in loose contact; 2 ˚C/min heating rate.

Figure 9. Combined soot oxidation and NO_x SCR in the physical mixture of KCP and Fe-ZSM-5. Reaction conditions: 500 ppm NO_x, 500 ppm NH_3, 4% O_2 in N_2; $NO_2/NO_x = 0$ for standard SCR and 0.5 for fast SCR; *w/f* 27 $g_{cat}\cdot$s/L; catalyst: soot mass ratio 9:1 in loose contact; 2 ˚C/min heating rate.

Figure 10. Combined soot oxidation and NO_x SCR in the physical mixture of KCP and Cu-ZSM-5. Reaction conditions: 500 ppm NO_x, 500 ppm NH_3, 4% O_2 in N_2; $NO_2/NO_x = 0$ for standard SCR and 0.5 for fast SCR; *w/f* 27 $g_{cat}\cdot$s/L; catalyst: soot mass ratio 9:1 in loose contact; 2 ˚C/min heating rate.

Figure 11. N_2O production during the combined soot oxidation and NO_x SCR in the physical mixture of soot oxidation and SCR catalysts. Reaction conditions: 500 ppm NO_x, 500 ppm NH_3, 4% O_2 in N_2; $NO_2/NO_x = 0$ for standard SCR and 0.5 for fast SCR; *w/f* 27 $g_{cat}\cdot$s/L; catalyst: soot mass ratio 9:1 in loose contact; 2 ˚C/min heating rate.